Dynamic Design and Simulation Analysis of Permanent Magnet Motor in Different Scenario of fed Alimentation

Article · August 2013

2 authors:

Hacene Mellah
Université de Bouira
45 PUBLICATIONS **91** CITATIONS

SEE PROFILE

Kamel Eddine Hemsas
Ferhat Abbas University of Setif
73 PUBLICATIONS **389** CITATIONS

SEE PROFILE

Some of the authors of this publication are also working on these related projects:

Project   Modeling based on tests of Frequency Response Analysis (FRA) for the analysis, monitoring and diagnosis of the dynamic behavior of power transformers View project

Project   Free & Online International Conference on Modern Electrical Engineering and Technology (ICMEET) View project

Dynamic Design and Simulation Analysis of Permanent Magnet Motor in Different Scenario of Fed Alimentation

Mellah Hacene [*1], Hemsas Kamel Eddine [2]

Electrical machine Department Ferhat Abbas University, Setif 1, cite maabouda 19000, Algeria

Automatic laboratory (LAS), Electrical engineering department, Ferhat Abbas University, Setif 1, Algeria

[*1] has.mel@gmail.com; [2] hemsas_ke@gmail.com

Abstract- **This paper deals with investigation on non purely sinusoidal input supply analysis of line-start PMM using finite element analysis (FEA), in the present times a greater awareness is generated by the problems of harmonic voltages and currents produced by non-linear loads like the power electronic converters. These combine with non-linear nature of PMM core and produce severe distortions in voltages and currents and increase the power loss, additional copper losses due to harmonic currents, increased core losses, electromagnetic interference with communication circuits, efficiency reduction, increased in motors temperature and torque oscillations. In addition to the operation of PMM on the sinusoidal supplies, the harmonic behavior becomes important as the size and rating of the PMM increases. Thus the study of harmonics is of great practical significance in the operation of PMM.**

Keywords- Permanent Magnet Machine; FEA; Non-Sinusoidal Supply, Harmonic; FFT; Loss

I. INTRODUCTION

In a modern industrialized country about 65% of electrical energy is consumed by electrical drives. Constant-speed, variable-speed or servo-motor drives are used almost everywhere: in industry, trade and service, house-holds, electric traction, road vehicles, ships, aircrafts, military equipment, medical equipment and agriculture [1]. Permanent magnet (PM) machines provide high efficiency, compact size, robustness, lightweight, and low noise, [2], [3], these features qualify them as the best suitable machine for medical applications [2]. Without forgetting its simple structure, high thrust, ease of maintenance, and controller feedback, make it possible to take the place of steam catapults in the future [3]. Most of the low speed wind turbine generators presented is permanent-magnet (PM) machines. These have advantages of high efficiency and reliability, since there is no need of external excitation and conductor losses are removed from the rotor [4].

Recent studies show a great demand for small to medium rating (up to 20 kW) wind generators for standalone generation-battery systems in remote areas. The type of generator for this application is required to be compact and light so that the generators can be conveniently installed at the top of the towers and directly coupled to the wind turbines [4]. The PM motor in an HEV power train is operated either as a motor during normal driving or as a generator during regenerative braking and power splitting as required by the vehicle operations and control strategies.

PM motors with higher power densities are also now increasingly choices for aircraft, marine, naval, and space applications [5].

The most commercially used PM material in traction drive motors is neodymium–ferrite–boron (Nd–Fe–B) [6]. This material has a very low Curie temperature and high temperature sensitivity. It is often necessary to increase the size of magnets to avoid demagnetization at high temperatures and high currents [6]. On the other hand, it is advantageous to use as little PM material as possible in order to reduce the cost without sacrificing the performance of the machine. Numerical methods, such as finite-element analysis (FEA), have been extensively used in PM motor designs, including calculating the magnet sizes. However, the preliminary dimensions of an electrical machine must first be determined before one can proceed to using FEA. In addition, many commercially available computer-aided design (CAD) packages for PM motor designs, such as SPEED, Rmxprt [4],[5] and flux2D [7], require the designer to choose the sizes of magnets. The performance of the PM motor can be made satisfactory by constantly adjusting the sizes of magnets and/or repeated FEA analyses [5].

II. PM MACHINE DESCRIPTION AND DESIGN

The operation principle of electric machines is based on the interaction between the magnetic fields and the currents flowing in the windings of the machine. In this study, the distributed type windings are used in the all types of designed machines. It is desired that the MMF (magneto-motive force) produced by stator windings to be as sinusoidal as possible. Rotational Machine Expert (RMxprt) is an interactive software package used for designing and analyzing electrical machines, is a module of Ansoft Maxwell 12.1 [8].
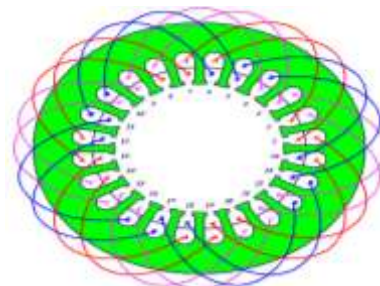

Fig. 1 Stator and coil structure of the designed motors

In this work, four poled rotor nub made up by NdFeB magnet material and stator nub with 24 slots coiled on copper conductor and spindle are used motors. The geometries of the motors are shown in Fig. 1.

The following table shows some design and operating parameters of PMSG used in our study.

Table I SOME RATED VALUES, GEOMETRIC PARAMETERS OF THE DESIGNED MACHINES

Parameter	Value
Rated Output Power (kW)	0.55
Rated Voltage (V)	220
Given Rated Speed (rpm)	1500
Type of Load	Constant Power
Number of Poles	4
Outer Diameter of Stator (mm)	120
Inner Diameter of Stator (mm)	75
Inner Diameter of Rotor (mm)	74
Length of Stator Core (Rotor) (mm)	65
Number of Stator Slots	24
Type of Magnet	NdFeB35
Type of Steel	Steel_1010
Stacking Factor of Stator Core	0.97
Width of Magnet (mm)	14
Stacking Factor of Iron Core	0.97
Thickness Magnet (mm)	3
Frictional Loss (W)	12
Operating Temperature (ÛC)	75

III. PERMANENT MAGNETS

Materials to retain magnetism were introduced in electrical machine research in the 1950s. There has been a rapid progress in these kinds of materials since then. The magnetic flux density in the magnets can be considered to have two components. One is intrinsic and, therefore, due to the material characteristic depends on the permanent alignment of the crystal domains in an applied field during magnetization. It is referred to as the intrinsic flux density characteristic of the PMs. The flux density component, known as intrinsic flux density, Bi, saturates at some magnetic field intensities and does not increase with the applied magnetic field intensity. The other component of the flux density in the magnet is due to its magnetic field intensity as though the material does not exist in the presence of the applied magnetic field or in other words, is a very small component due to the magnetic field intensity in the coil in vacuum Bh. Therefore, the flux density in the magnet material is given by [9]:

$$B_m = B_h + B_i \qquad (1)$$

The excitation component B_h is directly proportional to magnetic field intensity H, and given by:

$$B_h = \mu_0 H \qquad (2)$$

In all magnetic materials, this component is very small compared to the intrinsic flux density. Combining Eq. (1)

and Eq. (2), the magnetic flux density can be written as:

$$B_m = B_i + \mu_0 H \qquad (3)$$

A typical ceramic magnet's intrinsic and magnet flux densities are shown for the second quadrant in Fig. 2. The magnetic flux density in the second quadrant is a straight line and it can be represented in general as:

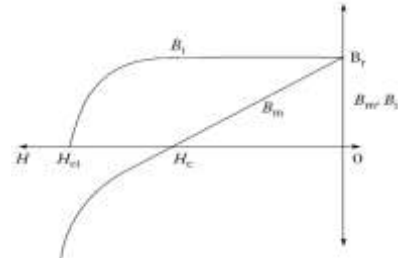$$B_m = B_r + \mu_0 \mu_{rm} H \qquad (4)$$

Fig. 2 Typical ceramic magnet flux densities

IV. SIMULATION RESULTS

A. Finite Element Mesh of the PMM

The finite element model is created. First, the geometric outlines are drawn, which is similar to the available mechanical engineering packages. Then, material properties are assigned to the various regions of the model. Next, the current sources and the boundary conditions are applied to the model. Finally, the finite element mesh is created. In the solver part, the finite element solution is conducted. The FEA model of electromagnetic field is built by Maxwell2D; in this case, the total number of mesh element is 1811.
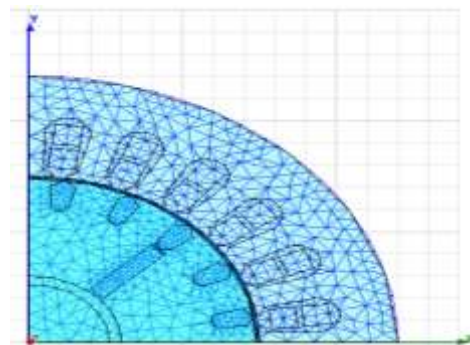

Fig. 3 Finite element mesh of PMM

The following sachems show the simulation schemas used to obtain our results, in the first case the LSPMSM is supplied with a pure sinusoidal, and even clearly the effects of harmonic we added each time a harmonic, in the second case the LSPMSM is supplied with a fed rich on harmonics, such as a triangular voltage.
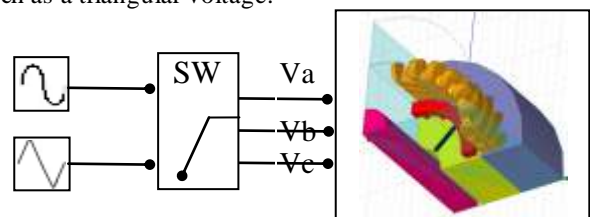

Fig. 4 Simulation schemes

The pure sinusoidal def can be written by:

$$\begin{cases} v_a = V_m \sin\left(\omega_s t + \varphi_1\right) \\ v_b = V_m \sin\left(\omega_s t + \varphi_1 - \dfrac{2\pi}{3}\right) \\ v_c = V_m \sin\left(\omega_s t + \varphi_1 + \dfrac{2\pi}{3}\right) \end{cases} \tag{5}$$

The addition of a 3th harmonic can be expressed mathematically by this equation:

$$\begin{cases} v_a = V_m \sin\left(\omega_s t + \varphi_1\right) + V_{3m} \sin\left(3\omega_s t + \varphi_3\right) \\ v_b = V_m \sin\left(\omega_s t + \varphi_1 - \dfrac{2\pi}{3}\right) + V_{3m} \sin\left(3\omega_s t + \varphi_3 - 3.\dfrac{2\pi}{3}\right) \\ v_c = V_m \sin\left(\omega_s t + \varphi_1 - \dfrac{4\pi}{3}\right) + V_{3m} \sin\left(3\omega_s t + \varphi_3 - 3.\dfrac{4\pi}{3}\right) \end{cases} \tag{6}$$

The addition of a 3th and 5th harmonic can be expressed mathematically by this equation:

$$\begin{cases} v_a = V_m \sin\left(\omega_s t + \varphi_1\right) + V_{3m} \sin\left(3\omega_s t + \varphi_3\right) + \\ \qquad\qquad V_{5m} \sin\left(5\omega_s t + \varphi_5\right) \\ v_b = V_m \sin\left(\omega_s t + \varphi_1 - \dfrac{2\pi}{3}\right) + V_{3m} \sin\left(3\omega_s t + \varphi_3 - 3.\dfrac{2\pi}{3}\right) \\ \qquad\qquad + V_{5m} \sin\left(5\omega_s t + \varphi_5 - 5.\dfrac{2\pi}{3}\right) \\ v_c = V_m \sin\left(\omega_s t + \varphi_1 - \dfrac{4\pi}{3}\right) + V_{3m} \sin\left(3\omega_s t + \varphi_3 - 3.\dfrac{4\pi}{3}\right) \\ \qquad\qquad + V_{5m} \sin\left(5\omega_s t + \varphi_5 - 5.\dfrac{4\pi}{3}\right) \end{cases} \tag{7}$$

If we take account the harmonic 3th, 5th and 7th, the power source can be represented as follows this:

$$\begin{cases} v_a = V_m \sin\left(\omega_s t + \varphi_1\right) + V_{3m} \sin\left(3\omega_s t + \varphi_3\right) + \\ \quad V_{5m} \sin\left(5\omega_s t + \varphi_5\right) + V_{7m} \sin\left(7\omega_s t + \varphi_7\right) \\ v_b = V_m \sin\left(\omega_s t + \varphi_1 - \dfrac{2\pi}{3}\right) + V_{3m} \sin\left(3\omega_s t + \varphi_3 - 3.\dfrac{2\pi}{3}\right) + \\ \quad V_{5m} \sin\left(5\omega_s t + \varphi_5 - 5.\dfrac{2\pi}{3}\right) + V_{7m} \sin\left(7\omega_s t + \varphi_7 - 7.\dfrac{2\pi}{3}\right) \\ v_c = V_m \sin\left(\omega_s t + \varphi_1 - \dfrac{4\pi}{3}\right) + V_{3m} \sin\left(3\omega_s t + \varphi_3 - 3.\dfrac{4\pi}{3}\right) + \\ \quad V_{5m} \sin\left(5\omega_s t + \varphi_5 - 5.\dfrac{4\pi}{3}\right) + V_{7m} \sin\left(7\omega_s t + \varphi_7 - 7.\dfrac{4\pi}{3}\right) \end{cases} \tag{8}$$

We represent the triangular supply in one period by this equation:

$$Va = \begin{cases} \dfrac{2v_m}{\pi} t & \text{, if } 0 < t < \dfrac{\pi}{2} \\ \dfrac{-2v_m}{\pi} t + 2v_m & \text{, if } \dfrac{\pi}{2} < t < \dfrac{3\pi}{2} \\ \dfrac{2v_m}{\pi} t - 4v_m & \text{, if } \dfrac{3\pi}{2} < t < 2\pi \end{cases} \tag{9}$$

$$Vb = \begin{cases} \dfrac{-2v_m}{\pi} t + v_m & \text{, if } 0 < t < \pi \\ \dfrac{2v_m}{\pi} t - v_m & \text{, if } \pi < t < 2\pi \end{cases} \tag{10}$$

$$Vc = \begin{cases} \dfrac{2v_m}{\pi} t - v_m & \text{, if } 0 < t < \pi \\ \dfrac{-2v_m}{\pi} t + 3v_m & \text{, if } \pi < t < 2\pi \end{cases} \tag{11}$$

B. Transient Results

Our designed machine by FE is supplied by different sources we presented before the simulation starts up to 1 second.

The FEA model of electromagnetic field is built by Maxwell2D, This simulation is obtained by Terra pc (QuadroFX380, i7CPU, 3.07GHZ, 8CPU, 4 G RAM.

1) LSPMSM Input Voltage Wave Form and Spectrum:

The first non ideality is the presence of harmonics in the sinusoidal input supply given to the three phase of LSPMM, in this case the source may contain 3th, 5th and 7th harmonics. We note that due to the symmetry, even ordered harmonics cannot exist [10].

Fig. 5a shows the input voltage wave form in the sinusoidal case, we can see that the fundamental magnitude is 311V and the frequency is 50Hz, in this figure we see that more than the voltage is polluted more than its form is distorted.

Fig. 5b shows the harmonic spectrum of the first simulation case
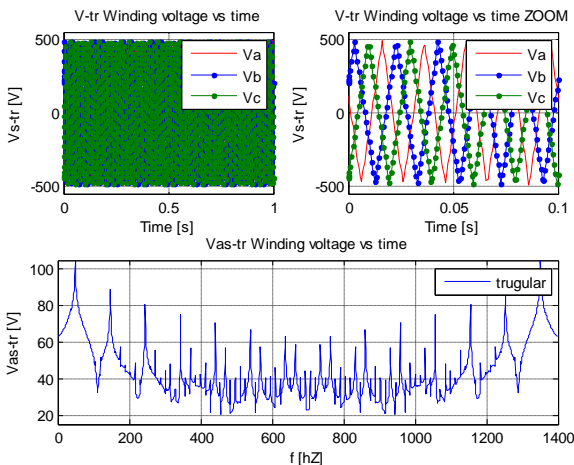
Fig. 5c shows triangular input voltage and their harmonic spectrum; the magnitude is 480V and the frequency is 50Hz.
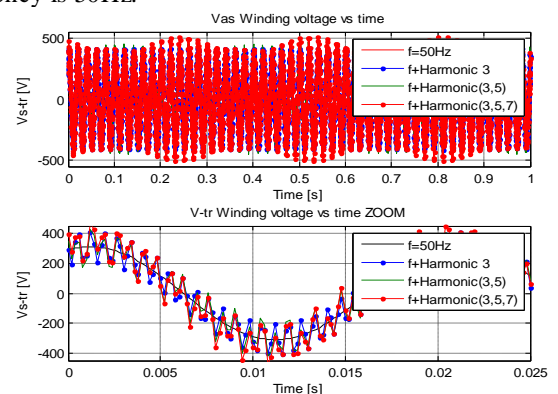
a. Sinusoidal input voltage.
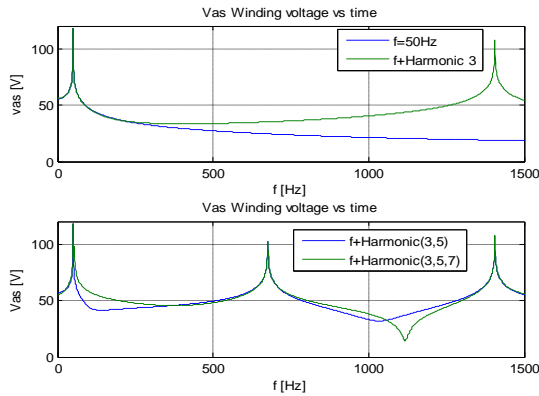
b. sinusoidal input voltage harmonic spectrum.

C. triangular input voltage and their harmonic spectrum

Fig. 5 PMM input voltage and their harmonic spectrum

By comparison between the Fig. 5b and the Fig. 5c, we note that more than the voltage rich in harmonic this form is deformed and deviate from the sinusoidal form.
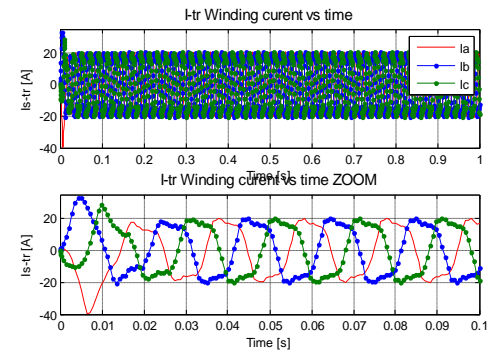
2) Winding Current Wave Form:

The starting current curve is indicated in Fig. 6, it can be seen that the rotational speed curve is steep at the pulling moment, and the motor can be pulled in synchronization preferably. Fig. 6a shows at starting the current value is 118A, but in study state reach the 16.25A for purely sinusoidal. Fig. 6b shows that more the signal is full with harmonic more than the spectrum of the signal is deformed. Fig. 6c shows that the current of phase follows the nature of the supply voltage.
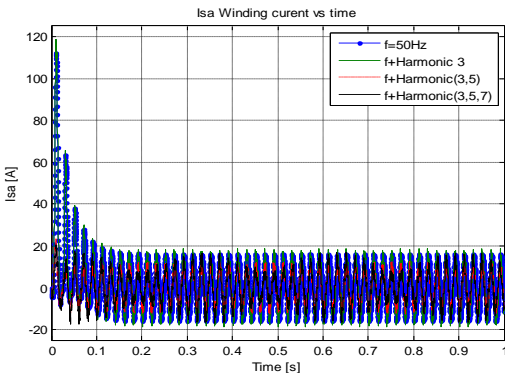
a. Winding current at sinusoidal fed.
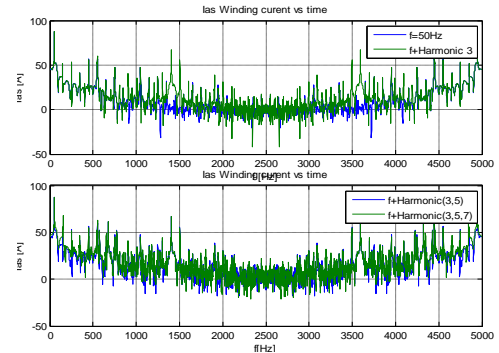
b. Winding current harmonic spectrum at sinusoidal fed.

a. winding current at triangular fed.

Fig. 6 PM machine current winding

3) Permanent Magnets Speed:

Rotational speed curve under rated load starting is presented in Fig. 7, the presence of the harmonics causes the appearance of the vibrations in Fig. 7a. Fig. 7b shows the speed curve in triangular fed, where it finds a peak reached the value 1650 rmp.
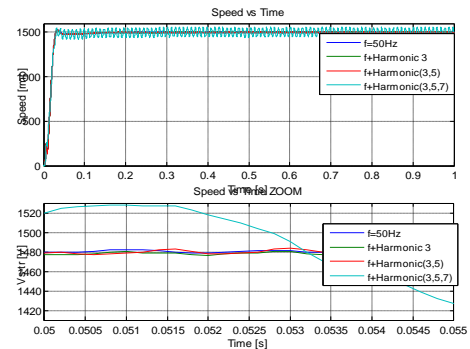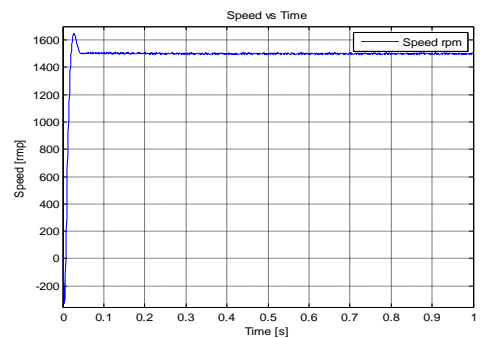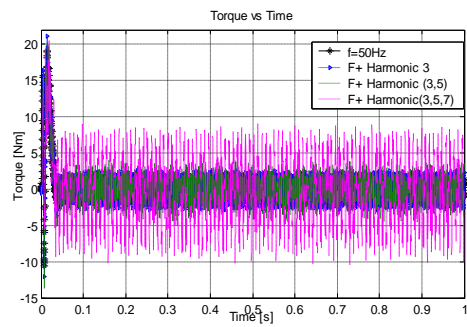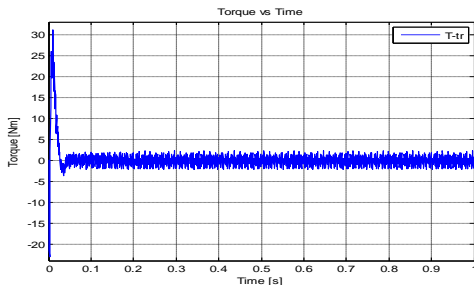

a. Sinusoidal

b. Triangular

Fig. 7 Speed in PM machine

4) Permanent Magnets Torque:

a. Sinusoidal

b. Triangular

Fig. 8 Torque in PM machine

Fig. 8 shows the electromagnetic torque curve under rated load starting, at that time, the starting torque is mainly determined by the asynchronous torque which is produced by rotor. After starting at 0.15 s, the motor is pulled in synchronization. The asynchronous torque disappears, and the electromagnetic torque is mainly afforded by permanent magnets. Motor is operating at synchronization state.

5) PMM Stranded and Solid Loss [11]:

Stranded Loss: Stranded loss is calculated for transient solution types. Stranded loss will be calculated for the following three cases:

Winding with voltage excitation and non-zero resistance:

$$S\_Loss = I^2 R \qquad (12)$$

Stranded current excitation with conductivity:

$$S\_Loss = I^2 / \sigma A \qquad (13)$$

External circuit, voltage source and non-zero resistance, thus here the dc resistance (calculated with the conductivity of the material of the respective cross section A) is used to calculate the stranded loss but not used in the circuit equation where it doesn't impact the current calculation (current is calculated taking R into account but not R(dc)).
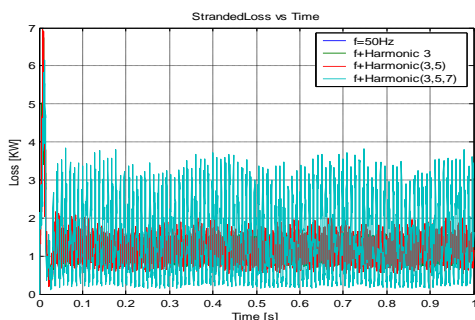
a. Stranded Loss at sinusoidal
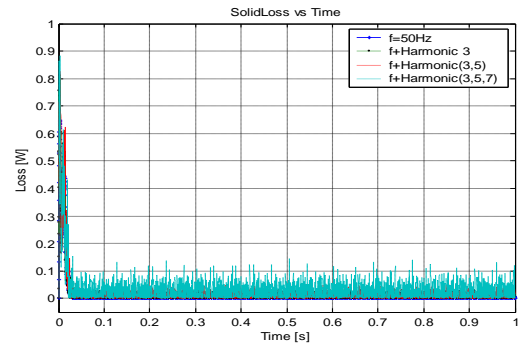
b. Stranded Loss at sinusoidal fed
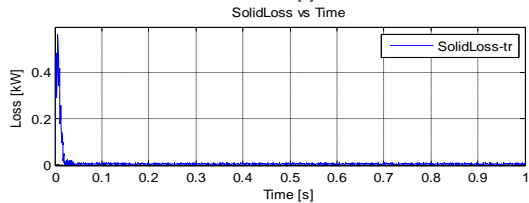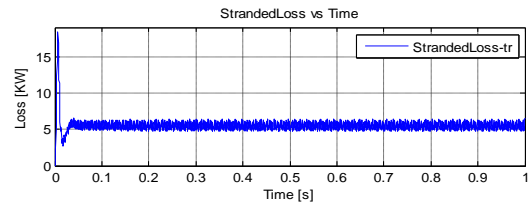
c. Stranded Loss and Solid Loss at triangular fed

Fig. 9 Stranded Loss and Solid Loss in PM machine

Solid Loss: the solid loss represents the resistive loss in a 2D or 3D volume and is calculated by:

$$Solid\ Loss = \frac{1}{\sigma} \int_{vol} J^2 \qquad (14)$$

6) FEA Analysis of Transient Electromagnetic Field:

The FEA model of electromagnetic field is built by Maxwell2D, the flux, flux density, magnet field intensity.

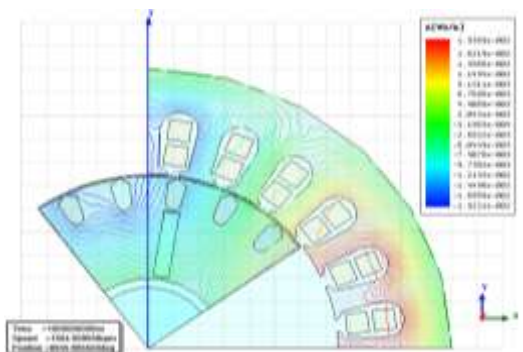Fig. 9 indicates the flux line distribution of the PMM at 1s.

Fig. 10 Flux distribution of PM machine at 1s

Fig. 11a, Fig. 11b show vector diagram of flux density in sinusoidal and triangular fed at 0.2s respectively. According to Fig. 11a, Fig. 11b, flux line and magnetic field are symmetrical in the whole motor. The distribution regularities of flux line and magnetic field are the same.
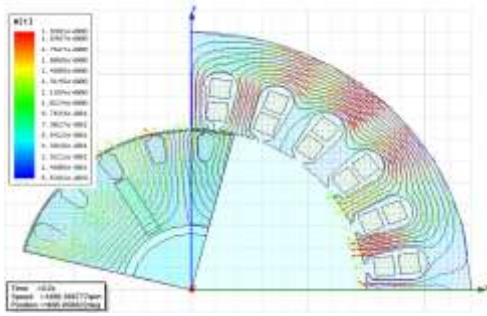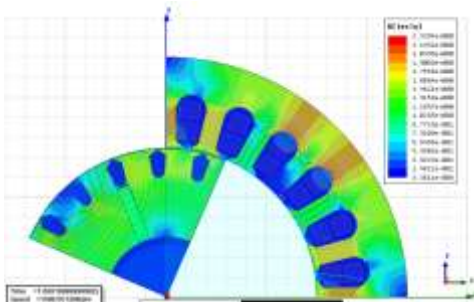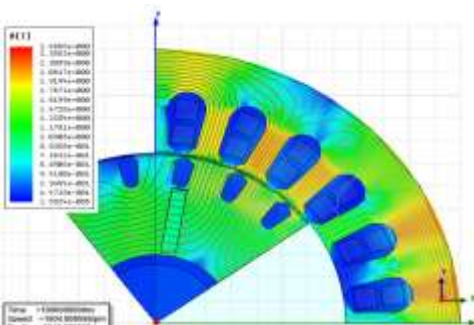
a. Sinusoidal
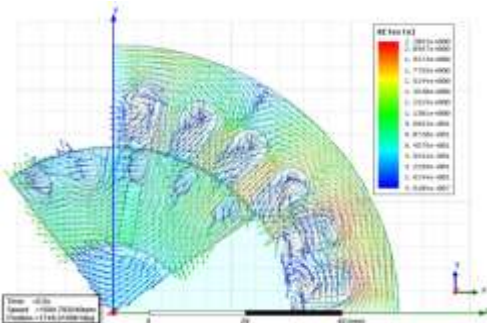
b. Triangular.

Fig. 11 Vector diagram of flux density in sinusoidal and triangular fed at 0.2s

Fig. 12 shows the flux line and contours diagram of flux density at sinusoidal and triangular fed at 1s respectively. The maximum value of flux density at 1s is bigger than 0.2s at triangular and sinusoidal fed, and the maximum value of flux density at sinusoidal fed is smaller than triangular feds.
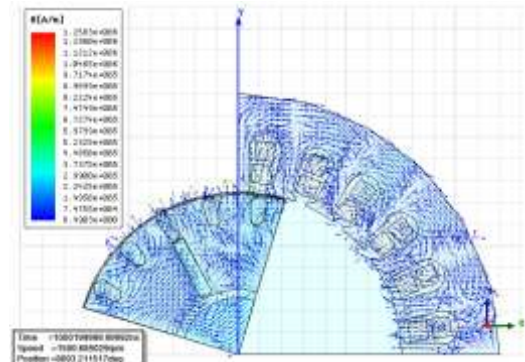

a. Sinusoidal

b. Triangular.

Fig. 12 Contours diagram of flux and flux density in sinusoidal and triangular fed

The following table summarizes the precedent results and gives the maximum values of flux density in steady and transient state for the sinusoidal and triangular supplies.

TABLE II MAXIMUM VALUE OF FLUX DENSITY

Time	0.2s	1s
Sinusoidal fed (B_{max}[T])	1.9961	2.3394
Triangular (B_{max}[T])	2.2063	2.4666

Fig. 13a and Fig. 13b show the vector of magnet field intensity at sinusoidal and triangular fed at 1s respectively. The relationship between the magnetic flux density and the magnetic field intensity represented by the demagnetization curve only exists when the magnetic field intensity varies in the same direction see Fig. 14.

a. Sinusoidal
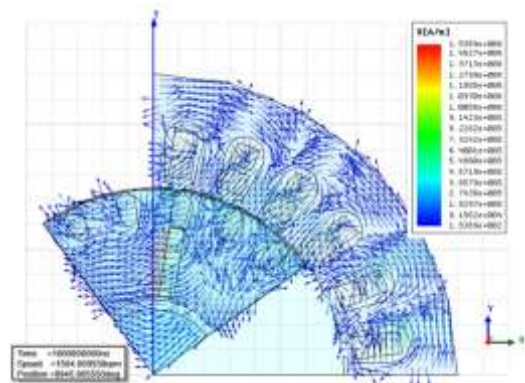
b. Triangular

Fig. 13 Magnetic field intensity at sinusoidal and triangular fed PM machine

In fact, when the permanent magnet electric machine is working, the demagnetization field intensity varies repeatedly in both directions.
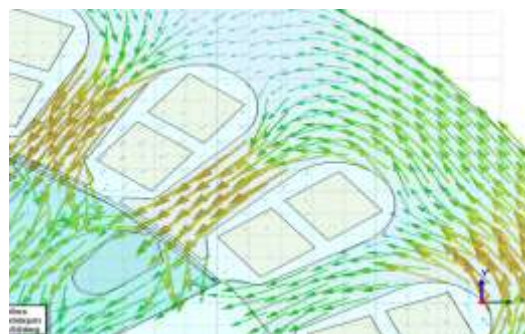

Fig. 14 H and B Zoom in Triangular fed PMM

Fig. 14 shows a part of the permanent magnet flux is canalized into the iron sections, when the stator current is applied.

V. CONCLUSION

This work is the necessary preparations for design and development high reliability and high security of PMM applications.

The paper shows finite element numerical result is consistency for magnetic field characteristics of permanent magnet machine under different scenarios of supply alimentation. Using Ansoft finite element software can be used as an effective way to design and calculate the new unbalanced fed machine.

As the harmonics in the voltage source can cause excessive losses, extra noise and pulsating torque detecting harmonics in the voltage applied is important. The frequency analysis of the stator currents can be used for detection. In the case of unbalanced voltages the efficiency and average output torque of the machine would decrease and the ripple would increase significantly destructing the machine application.

REFERENCES

[1] F. JACEK, Permanent Design and Applications, Second Edition, Revised and Expanded United Technologies Research Center Hartford, Connecticut London, United Kingdom 2002.

[2] A. Nasiri, Salaheddin A. Zabalawi, and Dean C. Jeutter, A Linear Permanent Magnet Generator for Powering Implanted Electronic Devices, IEEE transactions on power electronics, pp. 192–199, vol. 26, no. 1, Jan. 2011.

[3] L. Li, H. Junjie, L. Zhang, Y. Liu, S. Yang, R. Liu, L. Xiaopeng, "Fields and Inductances of the Sectioned Permanent-Magnet Synchronous Linear Machine Used in the EMALS," IEEE Transactions on Plasma Science, pp. 87-93, Vol. 39, Jan. 2011.

[4] İ. Tarımer, C. Ocak, "Performance Comparison of Internal and External Rotor Structured Wind Generators Mounted From Same Permanent Magnets on Same Geometry," Electronics And Electrical Engineering, pp. 1392 – 1215, 2009.

[5] C. Mi Chunting, Analytical Design of Permanent-Magnet Traction-Drive Motors; IEEE Tansactions on Magnetics, vol. 42, no. 7, July 2006.

[6] M. Haavisto, H. Kankaapaa, and Martti Paju, Estimation of Time-Dependent Polarization Losses in Sintered Nd-Fe-B Permanent, IEEE Transactions on Magnetics, vol. 47, no. 1, January 2011.

[7] P.P. de Paula, S.I. Nabeta, A. Foggia, "An aspect of modelling a permanent magnet motor by using the finite-element method coupled with circuit equations," IEEE Conference Publications Electric Machines and Drives, International Conference IEMD '99, pp. 135–137, May. 1999.

[8] Y. Wang, Y. Wang, H. Qiu, X. Liu, "Dynamic design and simulation analysis of 1000MW large turbo-generator, IEEE Conference Publications, International Conference on Mechatronics and Automation ICMA," pp. 1650–1655, Aug. 2009.

[9] R. Krishnan, Permanent Magnet Synchronous and Brushless DC Motor Drives, Taylor and Francis Group, LLC 2010.

[10] P. Barrade, Electronique de puissance, Méthode et convertisseurs élémentaires, presses polytechniques et universitaires romandes, 2006.

[11] Help of Ansoft Maxwell V12®, Ansoft Corporation 2010.